

Evaluating the Viability of Bioprinting Skin Organotypic Through a Comparison of the Contraction of Collagen Hydrogels Prepared Using Extrusion-Based Printing and Traditional Skin Grafting Methods

Abstract:

Bioprinting techniques currently have the ability to eliminate the need for donors and allow for faster integration with host tissue. However, the shear force applied during printing presents the potential to damage cells. During our experiment, we aimed to evaluate the cell survivability rates of fibroblasts. One of the most essential components of artificial skin constructs is the fibroblasts, which synthesize collagen and the extracellular matrix. In order to test the viability of this component once passed through the bioprinter nozzle, the collagen contraction was observed. The collagen gels were first prepared to have a concentration of 1.2 mg/mL and 7.5×10^4 cells/well for three poured and three printed samples. The associated volumes of materials including collagen and L-glutamine were combined along with cells to create a collagen gel solution. Three samples, each with a layer of collagen gel solution without cells and a separate layer with cells were printed at a pressure of 10 kPa. Three samples were also poured as a control to observe the effect of shear force on cell survivability. These gel inserts were then placed in the incubator at 37 °C to set. The contraction rate of the collagen gel was measured and compared over a period of 11 days using EVOS Imaging and Image J software. The results of the collagen contraction experiment showed that the contraction rates were very similar. Future research would include testing multiple trials and varying pressures to test the accuracy of these results.

Introduction:

Multiple tissue engineering methods have been applied to construct skin grafts for skin related injuries, such as burns, cuts, and lacerations, many of which require immediate treatment to avoid severe complications. However, several disadvantages accompany these currently utilized methods, including immune reactions, transmission of diseases, and shortages of donor skin. A novel technique - bioprinting - would alleviate many of these complications.[1] Bioprinting is a rapidly emerging field in regenerative medicine involving the production of cell-laden, three-dimensional structures that function to mimic bodily tissues. Bioprinting skin holds great potential for application in skin injury treatments as it would not only eliminate the need for donors through the production of regenerative scaffolds, but it would also prevent homogeneity issues accompanied by current methods. This is due to the fact that bioprinting allows for faster integration with the host tissue, lower risk of rejection, and, most importantly, uniform tissue growth in vivo. In addition, scientists would be able to have precise control of the process, providing access to patient-specific spatial geometry and controlled microstructures in the fabrication of tissue engineering scaffolds. Using bioprinting technology and the process of g-coding, scientists are able to create precisely planned skin grafts with skin cells that match those of the recipient.[2]

There are many different types of fabrication techniques regarding bioprinting, including laser-based, extrusion-based and inkjet-based bioprinting. Currently, extrusion-based printing is found to be the most feasible bioprinting technique in terms of vertical configuration and allowing usage of a larger variety of bioinks, including more cell-dense bioinks. However, present limitations include lower cell survivability due to the shear stress that is exerted on the bioink during printing. Shear stress poses the risk to damage cell membranes, cause cell apoptosis, and a decrease in living cells. [2] Furthermore, shear stress can negatively affect cell morphology and metabolic activity as well as cells' adhesiveness to the desired substrate.[3] Extrusion-based printing also allows for minimal substance control when printing. Bioprinting methods using Inkjet printers allow for precision and maximum control when printing substances into a petri dish. Rather than flowing out at a continuous rate, which is done through an extrusion-based printer, inkjet printers are similar to titration burettes and allow for controlled addition of substances

to petri dishes or other containers used. The severity of such effects, presented by the limitations of extrusion-based printing, depends on many factors including the viscosity of the bioink and cell types used. [2]

Promising results using extrusion-based printing have already been observed by previous experiments, showing that the risks posed by shear stress can be avoided and overcome. For example, in an experiment led by JS Lee, scientists were able to use an extrusion bioprinter to regenerate an ear with 95% cell viability.[4] These results drive our desire to conduct an experiment, evaluating the viability of cells through a measurement and comparison of collagen contraction rates between printed and poured values. During our experiment, we aim to evaluate the effect of shear stress on cell survivability and functionality of keratinocytes and fibroblasts, comparing the collagen contraction rates of poured and printed samples of a collagen gel solution. Keratinocytes and fibroblasts are important cellular components of skin, forming the extracellular matrix and the separate dermal layers. Keratinocytes mainly function in differentiation and fibroblasts, along with collagen in the extracellular matrix, function in contraction. By creating our hydrogels, which mimic skin, we should be able to test the functionality of these two cellular components, observing contraction rates and deducing cell survivability rates.

Materials/Methods:

Collagen Gel Preparation:

The collagen gels needed for this experiment were first prepared to have a final concentration of 1.2 mg/mL and a concentration of 7.5×10^4 cells/well for three printed and three plated samples. This process was started first through the combination of the associated volumes of each of the materials shown in *Table 1* to create a collagen gel solution that made up the first layer of our collagen gel. Our collagen gel consisted of three layers, the first of which was

Component:	Per 5 mL:	Per 13 mL
10x EMEM	0.5 mL	1.3 mL
L. Glutamine	0.0416 mL	0.10816 mL
FBS	0.5 mL	1.3 mL
Na ₂ CO ₃	0.142 mL	0.3692 mL
Collagen (4.82 mg/mL)	2.84 mL	7.384 mL
PBS (add until reach desired amount of mL)	Approximately 1 mL	Approximately 2.6 mL
NaOH	Until a pH of 7---red	Until a pH of 7---red

Table 1: Volumes of First Layer Collagen Gel Components

cell-deficient. After reviewing previous research done in this field and referencing multiple journal articles, the components needed for effective creation of a collagen hydrogel and their associated ideal volumes per 5 mL were implemented. These values were multiplied by a value of $\frac{13}{5}$ to acquire the necessary volumes for a total volume of 13 mL, 1 mL per well for 12 wells in addition to an extra mL for security. Using 5 mL and 1 mL pipette tips, each of the components of the first layer were accurately measured and combined in a 50 mL test tube for further preparation. These components were combined by consistently pipetting the solution, once in the test tube. This gel solution was then placed in the incubator at 37 °C to set.

The second layer of this collagen gel contained fibroblast cells at a concentration of 7.5×10^4 cells/well. This concentration of cells per well was achieved through the use of a manual cell isolation method. Initially, any medium in the given cell culture was removed using an aspirator and replaced with 1 mL of PBS, which was suctioned again. Cells were incubated at 37°C with trypsin to facilitate their removal from the bottom of the flask and then in DMEM medium, which is known to neutralize the trypsin. After a set period of time, the flasks were removed from the incubator and their components were transferred to a centrifuge tube. This tube was then placed in the centrifuge at 1200 rpm for 5 minutes to achieve maximum cell isolation from the medium. Once the cells settled to the bottom of the tube, the liquid is removed and the cells are counted under an optical microscope. This allows us to determine the amount of cells present per mL and further allows the addition of cells to the collagen solution with a cell concentration of 2.25×10^4 cells/mL. The volumes of the components shown in *Table 2* are combined just as they were for the first layer, however, with a higher total volume because for each well the second layer will consist of 3 mL of solution rather than 1 mL. Accounting for the 12 wells, approximately 36 mL of this solution are made. Combining the appropriate

Component:	Per 5 mL:	Per 36 mL
10x EMEM	0.5 mL	3.6 mL
L. Glutamine	0.0416 mL	.29952 mL
FBS	0.5 mL	3.6 mL

amounts of each component and adding the cells, the resulting solution is poured on top of the gelled first layer. This gel solution was then placed in the incubator at 37 °C to set for 2 days.

The third and final layer of this collagen gel was prepared through the use of washers and keratinocyte cells. The keratinocytes were prepared by removing the medium from the given flask with keratinocytes and 3T3 cells using the aspirator and replacing it with 5 mL of PBS with edta to remove the 3T3 cells from the flask. This liquid is then suctioned and replaced with trypsin to remove any cells stuck on the bottom of the flask. For two days, the medium of the keratinocytes was changed daily, adding 4 mL of filtered K⁺ media after suctioning the old medium on day one with 160 microliters of JGI. At this time, 1 mL of the above solution was separated and centrifuged to determine cell concentration following the method used for the fibroblasts. After the ideal concentration of cells/mL was established, the keratinocytes were resuspended in 2 mL of medium to get the total number of needed cells. On day two, 160 microliters of JGII were added to 2 mL of medium and together they were filtered before replacing the old medium in the flasks. 50 microliters of this solution was then added to washers placed on top of each of the collagen gels in the wells, forming a third layer. This combine gel product was then placed in the incubator at 37 °C to set for a period of approximately two weeks, during which the media was changed every two days for the first week and then every day for the last week. When changing the media, after the old medium is suctioned using an aspirator, 3 mL of DMEM medium is added to the bottom of the well through the existing inserts and 2 mL of the same medium is added to the top of the gel. After sufficient cell growth and differentiation, the contraction rate of the collagen gel was measured and compared using EVOS imaging.

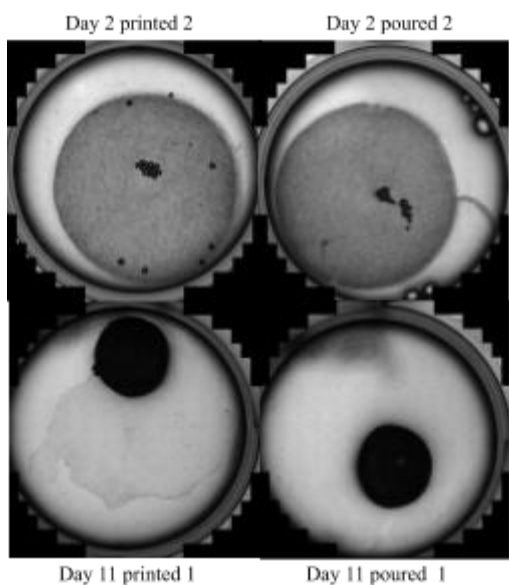


Figure 1: Images of collagen gels obtained through EVOS imaging using in determining the rate of collagen contraction

EVOS Imaging and Determination of Collagen Contraction Rates:

After the keratinocytes had sufficient time to differentiate and the collagen gel was fully set, the contraction rate of the collagen gel was measured and compared using EVOS imaging. For 11 days, images were taken of both the poured and printed samples using an EVOS Imaging computer software and imaging machine. Three images were taken of each type of sample on each day, each well scanned for approximately 15 minutes to obtain an accurately proportioned and visual image. Once each image was taken, they were all saved and put into a computer software, ImageJ, which was used to determine the average diameters of the collagen gel each of the 11 days. In order to accurately determine an average diameter for each image, a scale was first established. Using an image of one of the petri dishes used, the average diameter of the petri dish was determined. Five lines were drawn across the petri dish and the value of the distance between the endpoints of the lines were given in pixels. All five pixel values were then averaged to determine the average diameter in pixels. Using the

known diameter of the petri dish, which was 24 mm, a scale was determined to convert all future values from pixels to mm. This same method was followed. The diameter of the collagen on each day was method was used for each of the images obtained through EVOS imaging, allowing for the determination of diameter lengths per day and, ultimately, the change in diameter of the collagen gel over a period of 11 days.

Statistical Analysis:

In order to compare the rates of collagen contraction of the printed and poured samples, the values (average diameter) determined through ImageJ were used to determine the average area (mm²) of the collagen gels per day. These values were then plotted on a two-line graph, one line representing values for the printed samples and the

other representing values for the poured samples. Using this graph, the rates of contraction over the 11 day period were determined and then compared through a Two Sample t-test Assuming Unequal Variances. Using the Microsoft Excel Data Analysis Software, we calculated p values to determine whether or not the differences in the rates for printed and poured samples were significant. As a general note, we aspired for large p values (>0.05) because this signifies that the two rates present few differences.

Results:

After utilizing the EVOS Imaging Microscope to obtain our collagen images over a period of 11 days, illustrating the contraction of our collagen hydrogels during this time period, measured diameters determined using ImageJ

$$A = \pi\left(\frac{D}{2}\right)^2$$

Figure 2: Area formula used for contraction rate calculations where A=Area and D=Average Diameter

were implemented into the formula shown in *Figure 2* to calculate the area per day. Multiple diameters were measured per image to account for the irregularities in the shapes of our collagen hydrogels, many of which deviated from perfect circles. The average diameter per sample type per day was calculated by taking the average of the several diameters measured. The calculated area values were then graphed in a bar graph format to compare the contraction rates of the poured and printed samples over the 11 day period.

Once the area values were graphed over the 11 day period, as illustrated in *Figure 3*, we were able to compare the overall contraction rates for the poured and printed

collagen hydrogel samples. Significant contraction was seen for both sample types, indicating that the shear force of the bioprinter had a minimal effect on the functionality of the extracellular matrix, which consisted of collagen and

fibroblasts. The areas of the collagen gels changed at relatively equal rates as seen in *Figure 3*, indicating that cell survivability was relatively high for both samples and confirming our aspiration to observe very little damage to the cell components used in creating this collagen hydrogel through a complex bioprinting process. These results rejected our proposed hypothesis, confirming that the shear force of a bioprinter has a minimal effect on the functionality of skin components including fibroblasts, which are cells sensitive to membrane damage. However, in order to make an accurate conclusion based on the collected data, we must perform a statistical analysis to determine the statistical significance of the observed similarities in collagen contraction rates between the poured and printed samples.

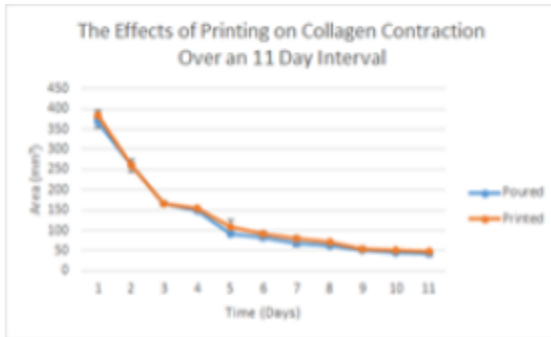


Figure 3: Comparison of collagen contraction rates between printed and poured hydrogel samples

Our statistical analysis was conducted through a Two Sample t-test

Assuming Unequal Variances, comparing the values for average area (mm²) covered and the contraction rates of printed and poured samples of the collagen hydrogels. This data analysis method was employed using Microsoft Excel Software, the data obtained through ImageJ, and our average area calculations. In completing this statistical

test we hoped for high p values greater than 0.05, which signify few differences in the contraction rates of the two samples. Although somewhat inconsistent, our statistical tests presented relatively high p values as shown in *Figure 4*, indicating that there are few differences between the printed and poured collagen contraction rates. Several of our data sets presented p values much larger than .05, however, a few select data sets presented p values much lower than this

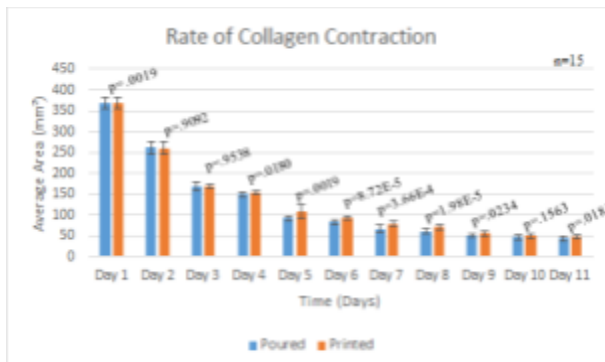


Figure 4: T-test two sample unequal variance statistical analysis

desired value. For this reason, our results, although significant in the field of biomedicine, may be inaccurate until confirmed with more experimental data or literature values.

Error Analysis:

There were many possible sources of error in our experimental procedure that may have interfered with our resulting data. For example, when pipetting our solution during the creation of collagen gels, slight bubbling occurred in some of the inserts. These bubbles remained prevalent throughout much of the experimental period and are even visible in many of our EVOS-produced images. Such air bubbles could have interfered with cell survivability and uniform hydrogel consistency, interfering with collagen contraction ability and allowing for inaccuracies in the resulting calculated values. In addition to the presence of bubbles on our gels, we noticed the presence of unknown “black dots” that may also have interfered with our data. We were unable to identify these particles, however, there is a high probability that they had an effect on the collagen contraction rates and the overall hydrogel functionality. Furthermore, the movement of collagen gels as they were transported between rooms in the lab could have caused damage to the cells. Cells are very fragile and any sudden or violent movements can cause damage. Moving between labs multiple times may have made the cells in both sample types susceptible to damage or even death.

Conclusion:

Our experiment aimed to evaluate the effect of the shear stress applied on cellular components of the collagen hydrogels during extrusion-based printing, observing the cell survivability rates of keratinocytes and fibroblasts by comparing poured and printed samples of a collagen gel solution. We found that the shear stress applied on these cells during bioprinting had a minimal effect on their functionality as there was significant contraction observed for both poured and printed samples. Neither sample presented signs of reduced cell survivability or collagen contraction. The statistical analysis somewhat confirms our deduction that bioprinting has a minimal damaging effect on the cellular components of skin. The resulting contraction rates were found to be very similar, suggesting that the functionality of skin components was not noticeably affected throughout the bioprinting process. However, there are many possibilities for inaccuracy in our data and we are unable to make any assertions until we proceed with similar experimental procedures.

Future directives include further research in which we would perform additional trials for more accuracy. As mentioned previously, the potential errors in our experimental procedure as well as the inconsistency in our statistical analysis suggest that our data is somewhat inaccurate. We would also aim to test varying amounts of pressure alongside the 10 kPa pressure value used in this experiment to evaluate the effect of varying amounts of shear stress exerted on the cells. Although future research must be conducted in order to further investigate the viability of bioprinting skin organotypic, our experiment yields promising results regarding the viability of bioprinting for future use in the field of biomedicine, contributing to making the use of bioprinting for treatment of patients a reality. Our experiment illustrates the potential of using bioprinting technology to produce homogenous and overall effective skin organotypics that may revolutionize skin grafting as it is done today.

References:

- [1] Augustine, Robin. “Skin bioprinting: a novel approach for creating artificial skin from synthetic and natural building blocks.” *Progress in biomaterials* vol. 7,2 (2018): 77-92. doi:10.1007/s40204-018-0087-0
- [2] Kačarević, Željka P et al. “An Introduction to 3D Bioprinting: Possibilities, Challenges and

Future Aspects.” *Materials* (Basel, Switzerland) vol. 11,11 2199. 6 Nov. 2018, doi:10.3390/ma11112199

[3] Falguni P., Jinah J., Lee J.W., Dong-Woo C. *Essentials of 3D Biofabrication and Translation*. Elsevier; Amsterdam, The Netherlands: 2015. *Extrusion Bioprinting*; pp. 123–152.

[4] Lee JS, Hong JM, Jung JW, Shim JH, Oh JH, Cho DW *Biofabrication*. 2014 Jun; 6(2):024103.